

Cryocooler Load Increase due to External Contamination of Low- ϵ Cryogenic Surfaces

R.G. Ross, Jr.

Jet Propulsion Laboratory
California Institute of Technology
Pasadena, CA 91109

ABSTRACT

An important challenge for the cryogenic system designer of space-instruments is achieving stable emittance values for low-emittance cryogenic surfaces that may be affected by condensed water films or other outgassing products over the life of a mission. Typically, low-emittance cryogenic surfaces get water films that increase in thickness over time and may lead to significant increases in the cryogenic heat load. If excessive load levels are reached, the cryogenic surfaces must be "defrosted" by raising them to elevated temperatures to evaporate the built-up contaminant films.

As a help to those designing and conducting future long-life missions with cryocoolers, this paper summarizes the applicable physics associated with surface contamination and compiles example flight data on contamination effects experienced during multi-year space missions and ground tests. The flight and ground test data are then compared with the physical parameters involved with contamination transport rates and the dependence of emittance on contaminant film thickness. Although the test sample is small, the data indicate that around a 10-20% load increase may be expected on-orbit due to contamination of low- ϵ surfaces. This level is found to be consistent with the sensitivity of emittance to film thickness and the expected contaminant levels in space.

INTRODUCTION

The cryogenic heat loads on a cryocooler can be roughly divided into three types: 1) Electrical power dissipation such as from a focal plane detector, 2) conductive parasitics down supports and electrical cables, and 3) radiation loads dependent on surface emittances and view factors of warmer objects that surround the cryogenic surfaces. In general, the electrical and conductive loads are relatively stable and predictable over the mission. However, the radiation loads are strongly dependent on surface temperatures and emittances that can change over time in less predictable ways. Key drivers for radiation loads are:

- The effective emissivity of the cryogenic surface area. Because the load is directly proportional to the emittance, very low emissivity levels ($\epsilon < 0.05$) can result in smaller loads. However, very small changes in the emittance ($\Delta\epsilon \approx 0.05$) will have a very large effect.
- The temperature of the warmer background that is radiating to the low-emissivity cryogenic surface. The radiation load varies as the fourth power of this background temperature.

- The total cryogenic surface area subject to radiation; the load is directly proportional to the total cryogenic surface area.

2

Given the above, the most sensitive parts of a cryogenic system will be high-surface-area parts at cryogenic temperatures that view high temperature surrounds, and utilize very low emittances to reduce the load. A difficult challenge faced by the cryogenic system designer is trying to achieve stable long-term emittances for these low-emittance surfaces as they are affected by contamination by condensed water films and outgassing products over the life of a mission.

THE PHYSICS CONTROLLING CONTAMINATION SENSITIVITY

As a precursor to examining measured rates of load increase in space, it is useful to first review the physics involved with contamination transport rates and the dependence of emittance on contaminant film thickness.

Effect of Contaminant Film Thickness on Emittance

Very thin deposited films of contaminant gases can significantly influence the emittance of low emittance surfaces such as polished gold or aluminum. Figure 1 describes the strong sensitivity of the emissivity of polished stainless steel to deposited films of various substances.¹ Note that thin films of water-ice have a particularly pronounced effect, increasing the emittance of the polished metal surface at an initial rate of around $\Delta\epsilon \approx 0.2$ per micrometer of water-ice thickness. Note also, that the emittance of water-ice films continues to increase and approaches unity at film thicknesses greater than 20 μm .

One can use these data to estimate the allowable film thickness for water-ice on a low emittance cryogenic surface. For example, for a polished gold surface with a nominal emittance of 0.05, a water-ice film thickness of approximately 1.0 micron would be expected to increase the emittance by two or three times, and thus greatly increase the radiative load.

Contaminant Film Transport Dynamics

Given that very thin deposited films of contaminant gases can significantly influence the emittance of low-emittance surfaces, the next issue is the rate that such films build up—in particular the rate dependence on the partial pressure of the contaminant gas that surrounds the target surface, and the surface temperature.

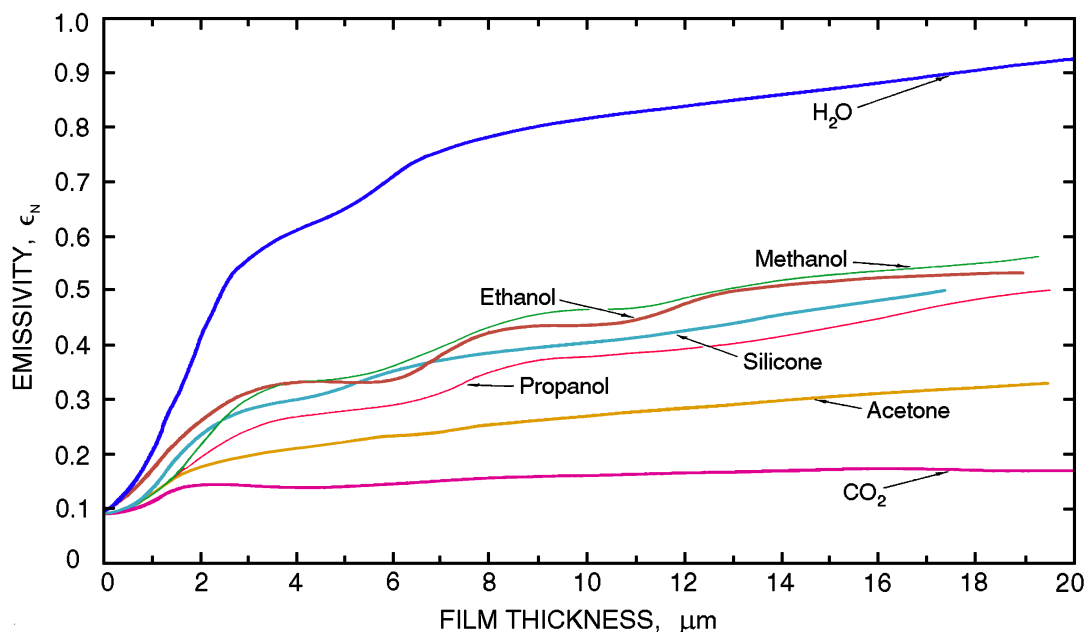


Figure 1. Emissivity of polished stainless steel at 77K versus film thickness of various frozen gases.¹

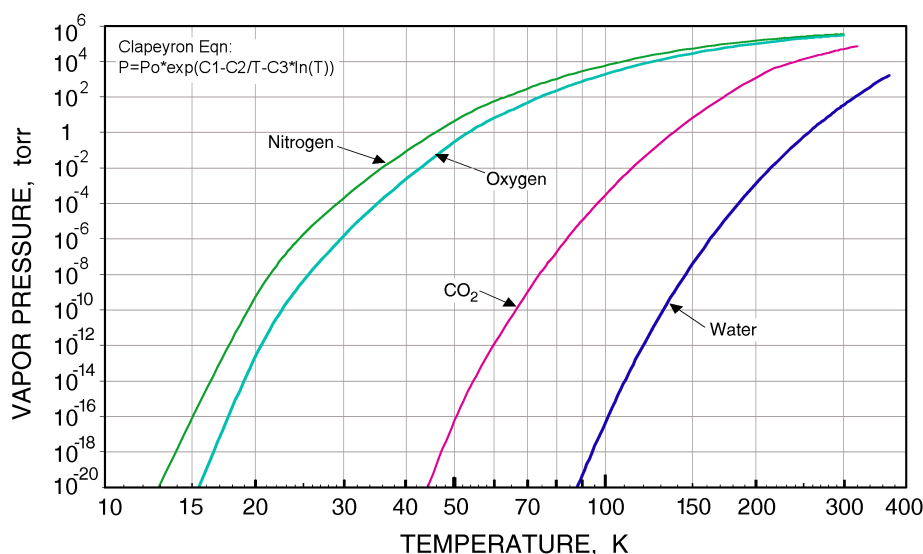


Figure 2. Saturation pressure curves of various gases (Claapeyron constants from Ref. 2).

Saturation Vapor Pressure. The saturation vapor pressure of a contaminant gas is the pressure at which the gas is in equilibrium with its solid or liquid phase at the same temperature. As noted in Fig. 2, the saturation vapor pressure of gases is a very strong function of temperature—spanning many orders of magnitude over the range of cryogenic temperatures. Of particular interest to the problem of surface contamination, a contaminant gas will build a meaningful film on a surface only if the gas' existing partial pressure is greater than or equal to its saturation pressure at the temperature of the cryogenic surface. By meaningful, we mean the film will develop enough thickness to have a measurable effect on the surface emittance. Virgin surfaces will adsorb and hold many monolayers of gas because the water-metal bond is much stronger than the water-water bond. However, the equilibrium thickness of these few monolayers is not sufficient to have a measurable effect on the surface emittance.

As an example, note in Fig. 2 that for a cryogenic surface at 145 K, a meaningful water film will deposit if the partial pressure of the surrounding water vapor is greater than 10^{-8} torr; likewise, no significant film will develop if the partial pressure is less than 10^{-8} torr. Or, from a cryopumping point-of-view, if one has an instrument enclosure at 145 K, the partial pressure of water vapor in the enclosure will be reduced to 10^{-8} torr by the cryopumping action of the enclosure walls.

Surface Residence Time. Another physical parameter associated with film development is surface residence time. This is the average time between when a molecule arrives on a surface and when it leaves the surface. In other words, it is a quantification of the ability of a molecular species to outgas from a particular surface at a particular temperature. Figure 3 illustrates the surface residence time involving two types of molecular bonds: 1) water-water bonds, and 2) water-metal bonds.³ Note that water is extremely tightly locked onto virgin metal surfaces below 250 K, but also to surface films of water below 100 K. For such surfaces the residence time is several years, and the surface film of water is essentially immobile. Thus, once water arrives on a cryogenic surface, it is very difficult for it to leave and migrate to another surface.

Predicting Typical Film Deposition Rates. For most applications involving cryocoolers, any cryogenic surfaces will be typically enclosed in a larger volume substantially warmer than the cryogenic surface itself. An example would be a cryocooler cold-tip enclosed in a room-temperature vacuum chamber, or a 60 K cryocooler cold-tip enclosed in a 150 K thermal shield. For such a case, the temperature of any residual gas in the volume will be approximately equal to the temperature of the chamber or shield wall, and any deposited film will be at the temperature of the cryogenic surface. Note from Fig. 3, that once a gas molecule hits a cryogenic surface, it is

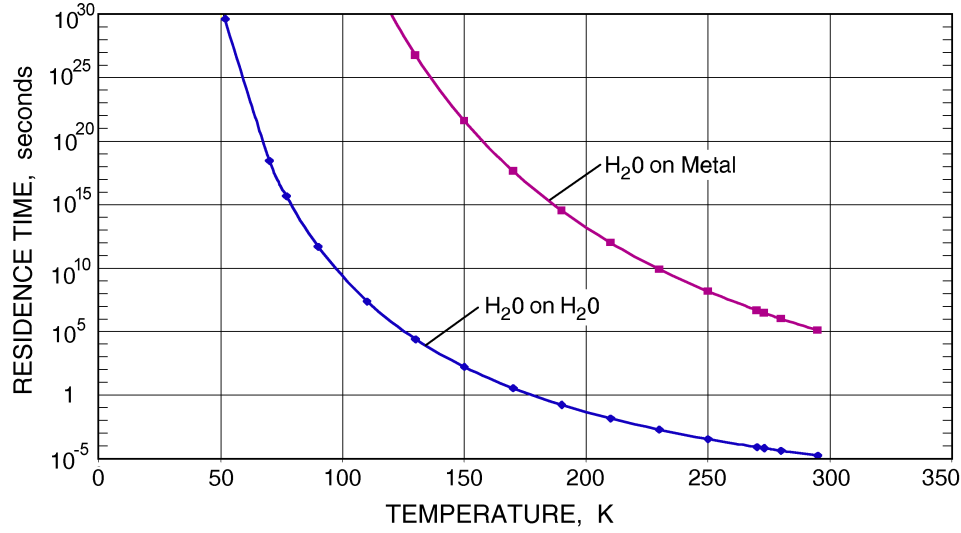


Figure 3. Residence time for water breaking water-water bonds and water-metal bonds.

unlikely to return to the surrounding gas. The rate at which molecules stick to the cryogenic surface and contribute to the film growth is referred to as the cryogenic pumping rate; this rate has been extensively modeled in the literature based on the kinetic theory of gases.^{4,5} For our case, the residual gas pressure is typically $> 10\times$ higher than the saturation gas pressure on the cryogenic surface, so the net mass flux collected by the cryogenic surface simplifies to:

$$\dot{m} = 5.83 \times 10^{-2} A P \sqrt{M/T} \quad (1)$$

where

- \dot{m} = rate of mass collected (g/sec)
- A = area of the cryogenic surface (cm²)
- P = external residual gas pressure (torr)
- M = molecular mass of the residual gas (e.g. $M=18$ for H₂O)
- T = external gas temperature (same as external wall temperature) (K)

Equation 1 also applies to the rate of sublimation from a surface where the saturation pressure of the surface is much higher than ($> 10\times$) the residual pressure in the surrounding volume. However, for this case T is the temperature of the cryogenic surface, and P is the film saturation pressure (from Fig. 2) corresponding to the temperature of the cryogenic surface.

To estimate the rate of film thickness buildup, or loss, we must divide by the film density and area; thus

$$\dot{\delta} = 5.83 \times 10^{-2} (P / \rho) \sqrt{M/T} \quad (2)$$

where

- $\dot{\delta}$ = rate of film thickness buildup (cm/sec)
- ρ = density of film (typical value for water ice is 0.9 g/cm³)

To quantify the issue for our application, consider a polished gold surface at 80 K surrounded by water vapor at a partial pressure $P = 10^{-5}$ torr and temperature of 300 K. For a cryogenic surface at 80 K, Fig. 2 indicates that the saturation pressure is many orders of magnitude below the residual gas pressure of 10^{-5} torr, so Eq. 2 is applicable, i.e., the rate of film deposition is completely determined by the external gas temperature and pressure. Substituting these values into Eq. 2 gives

$$\dot{\delta} = 5.83 \times 10^{-2} (10^{-5} / 0.9) \sqrt{18/300} = 3.74 \times 10^{-7} \text{ cm/s} = 0.0037 \text{ } \mu\text{m/s} \quad (3)$$

Thus, around 5 minutes would be required to build up a 1 μm film of water with a corresponding emittance increase of $\Delta\epsilon \approx 0.1$. Note that the rate of buildup is relatively independent of the cryogenic surface temperature once the saturation pressure at the surface temperature is well below the external vapor pressure.

As a second example, one can compute what external vapor pressure of water would be required to keep the deposited film thickness growth to 1 $\mu\text{m}/\text{year}$ ($3.17 \times 10^{-12} \text{ cm/s}$). Using Eq. 2 and solving for P gives:

$$P = 17.15 \delta \rho \sqrt{T/M} = 17.15 (3.17 \times 10^{-12} \text{ cm/s})(0.9)(300/18)^{0.5} = 2.0 \times 10^{-10} \text{ torr} \quad (4)$$

Thus, to achieve a long period without contamination, requires a very low residual partial pressure of water, or a high level of isolation of the cryogenic surfaces from the residual gas source.

Predicting typical film deposition rates where the gas source is isolated from the cryogenic surface. For many applications involving cryocoolers, the cryogenic surfaces are carefully sealed off from sources of external contaminants using multilayer insulation or physical barriers. For such applications it is useful to understand how well the sealing must be to achieve a desired film deposition rate. For the typical case where the pressure outside the restriction is much greater than ($> 10\times$) that near the cryogenic surface (the low pressure volume), we find that Eq. 1 again applies, but with the following change in definitions

$$\dot{m} = 5.83 \times 10^{-2} A P \sqrt{M/T} \quad (5)$$

where

- \dot{m} = rate of mass passing through an orifice into the low-pressure volume (g/sec)
- A = area of the orifice (cm^2)
- P = gas pressure outside the orifice (external source pressure) (torr)
- M = molecular mass of the gas (e.g. $M=18$ for H_2O)
- T = gas temperature outside the orifice (external source temperature), K

Comparing Eq. 5 with Eq. 1 indicates that the mass flow rate and film buildup rate are reduced proportional to the area ratio of the orifice area to the cryogenic surface area. Thus, a $\times 100$ rate reduction can be achieved by restricting access to the volume containing the cryogenic surface via an orifice with an area of 1% of the cryogenic surface area.

Emittance Degradation with Multilayer Insulation (MLI). For many applications involving cryocoolers, the low emittance surface is achieved using blankets made up of multi-layers of aluminized Mylar with internal spacer scrims to minimize direct film-to-film conduction. The various layers of the MLI thus operate as a stacked series of radiation shields at progressively increasing temperatures — from the cryogenic surface temperature to the surround temperature. Analyzing the effect of surface contamination on MLI is beyond the scope of this article, but the physics involved is the same, with the considerably added complexity of quantifying the water vapor migration rate through the MLI to get to the layers that are below the vapor's saturation temperature. Thus, the MLI acts as both a series of low emittance surfaces, plus a gas migration barrier to slow the deposition rate of contaminant films on the layers that are sufficiently cold. Unfortunately, the higher temperature layers of MLI blankets also serve as a considerable source of trapped surface moisture, and thus serve as a source of the water vapor capable of condensing on cold instrument optical and low-emittance surfaces.⁶

FLIGHT EXPERIENCE

Although the above theoretical background illuminates the physics behind the contamination of low-emittance cryogenic surfaces, there are a number of parameters that remain unquantified in practice. These include such things as:

- What is the background partial pressure of water in space in the interior of an instrument, and how does it vary over the course of a long-term mission?
- What sort of typical emittance changes or cryogenic load increases are seen over a long-term space mission?

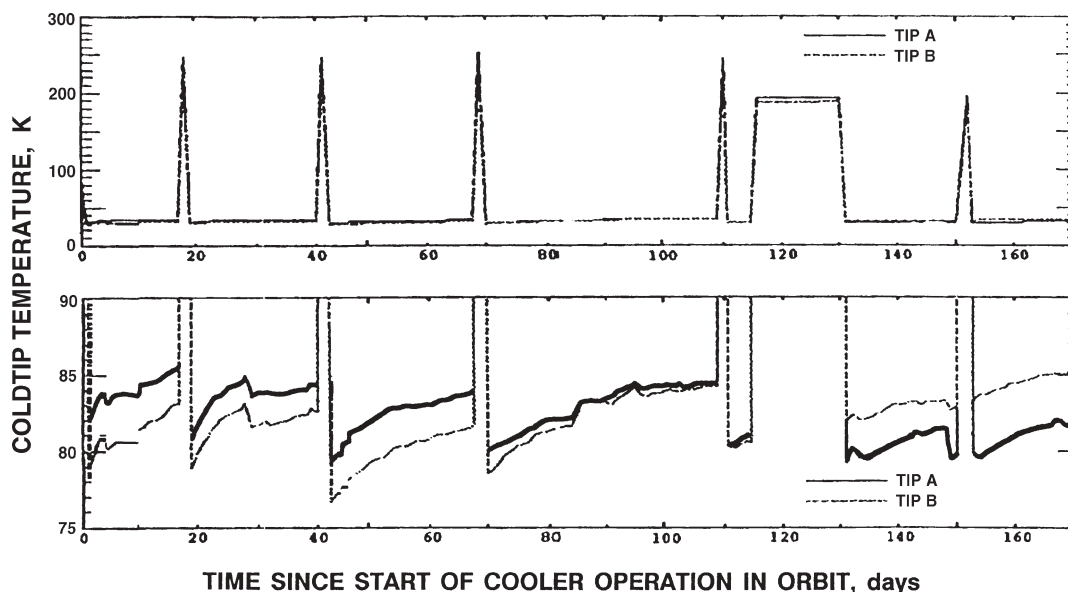


Figure 4. Coldtip temperature history for the ISAMS instrument aboard the UARS spacecraft.⁷ Vertical excursions are decontamination cycles where the instrument was heated to near room temperature to outgas the contaminants that were gettered to the instrument's cold surfaces.

To shed some light on these questions this section examines available data on the contamination effects experienced during multi-year space missions and laboratory life tests carried out over several months.

ISAMS Flight Experience

One of the first large cryocooled instruments in space was the Improved Stratospheric and Mesospheric Sounder (ISAMS) instrument that was launched aboard the Upper Atmospheric Research Satellite (UARS) platform in September 1991. This application utilized two Oxford 80 K cryocoolers running at ~83% stroke to hold a number of cryogenic detectors near 80 K. Figure 4 highlights the cryogenic temperature increase experienced by this instrument.⁷ Immediately after turn-on in orbit, it can be seen that the temperature of the detectors increased by around 5 K (from 80 to 85 K) over a three-week period. This temperature increase, which is considered to be the result of contamination gettered onto the cold plumbing's low-emittance surfaces, necessitated conducting a number of high-temperature decontamination cycles. Over time, the level of contamination slowly subsided, and after a year in orbit, the time required to reach a five-degree ΔT gradually increased to 2-3 months. This decrease over time confirms that the contamination was external-to and not internal-to the cryocooler.

To estimate the level of load increase associated with the 5 K ΔT one can appeal to the performance curves⁸ for the 80 K British Aerospace (BAe) cooler shown in Fig. 5. From these curves it is seen that a temperature change from 80 to 85 K at a constant piston stroke (83% of 8 mm = 6.64 mm) equates to a load increase of around 100 mW per cooler, or a 12% increase in the total cryogenic load. Understanding the actual level of emittance increase would also be useful, but the data needed for this calculation were not available to this author.

MOPITT Flight Experience

As a second example, the Measurements Of Pollution In The Troposphere (MOPITT) instrument initiated operation in March 2000 aboard the NASA EOS Terra spacecraft.⁹ This instrument uses two back-to-back BAe 50-80 K coolers to cool two detectors: #1 at around 92 K, and #2 at around 85 K. The instrument uses closed-loop control of the cooler stroke to maintain the #1 coldtip at a constant 78 K to control the #1 detector temperature, while the second cooler is forced to match the stroke of the first to maintain vibration control; the second cooler's cold-tip temperature thus varies somewhat.

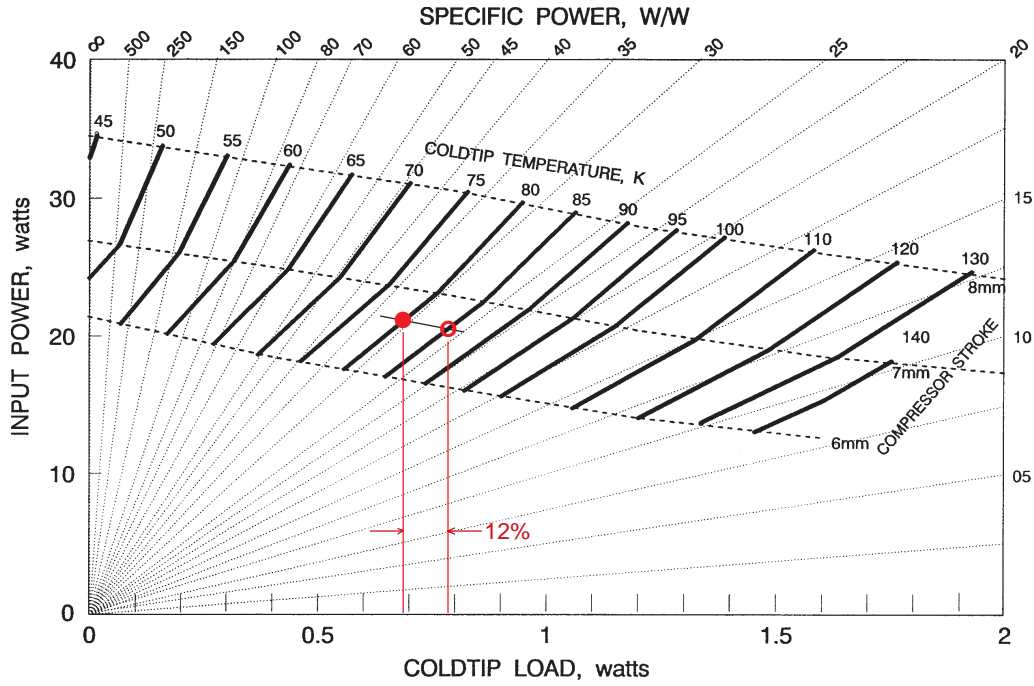


Figure 5. ISAMS warm-up data⁷ superimposed on representative performance⁸ of a BAe 80 K cryocooler plotted versus coldtip temperature, stroke, and input power for a 300 K heatsink temperature.

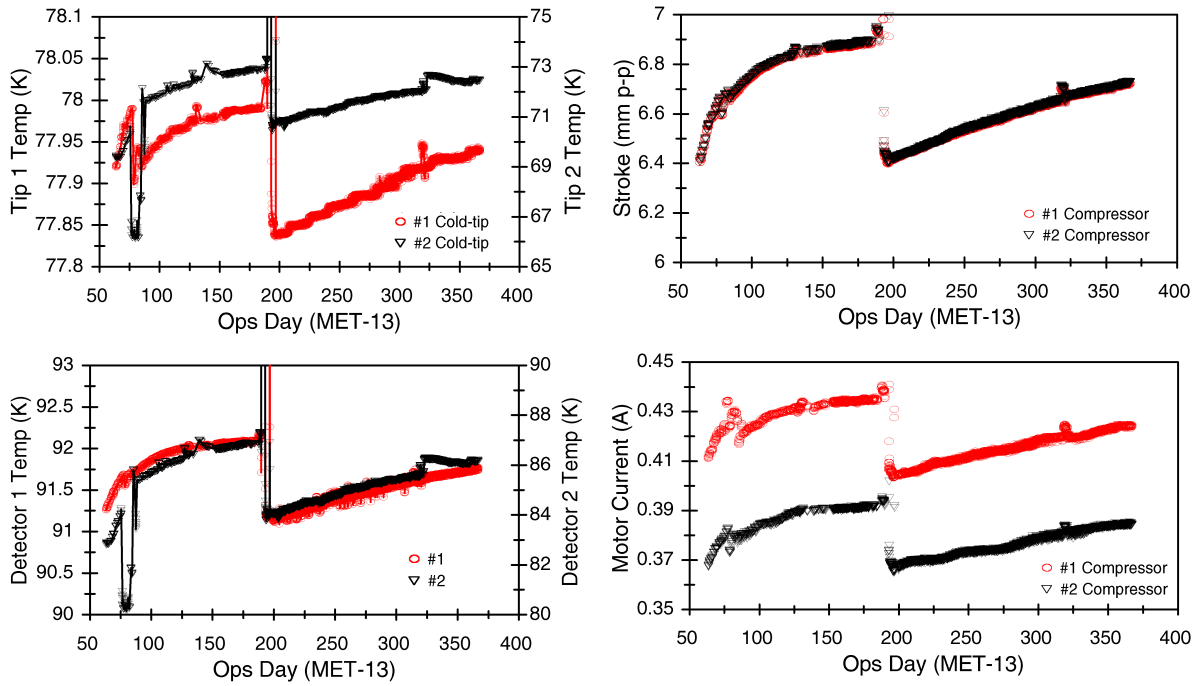


Figure 6. Cryocooler-coldtip and detector temperature and compressor stroke and current history for MOPITT instrument from beginning of mission to Ops day 370.¹⁰

Figure 6 describes the stroke and temperature history of the MOPITT coolers during the first year of mission operation.¹⁰ Note the decontamination warm-up cycle that was carried out around day 190 to recover gradual deterioration of the instrument's science quality. During the first part of the mission it can be seen that the cooler stroke increased from 6.4 to 6.9 mm p-p to carry the gradually increasing cryogenic load. After the decontamination cycle, the load fully recovered to its original value and the cooler stroke returned to 6.4 mm. Note also that contamination after the warm-up cycle reoccurred at a much slower rate than the original contamination, thus confirming that the contamination was external to the cryocooler.

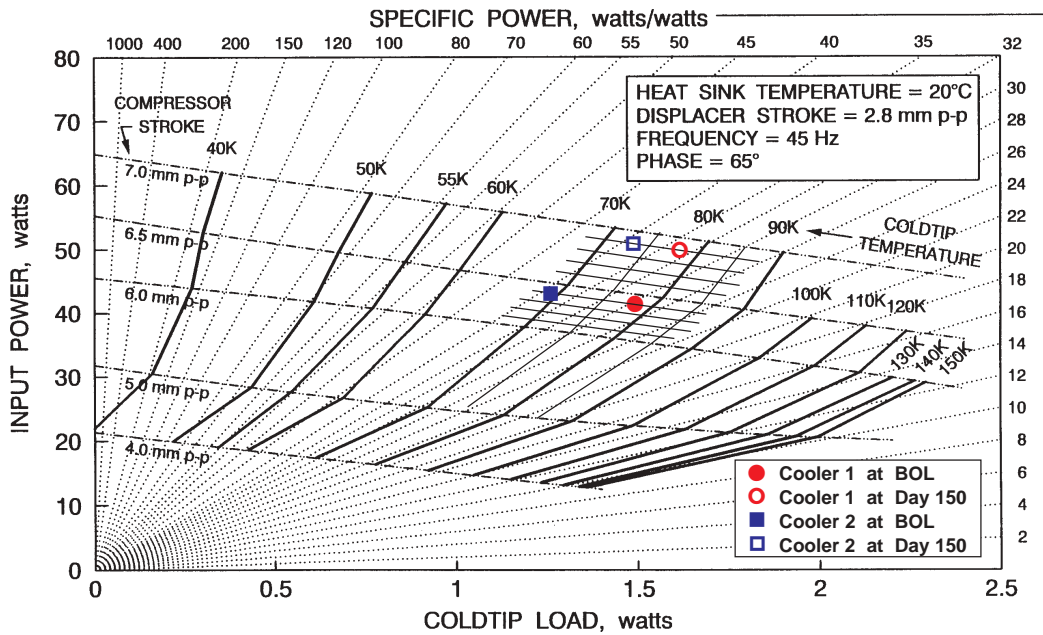


Figure 7. MOPITT cryocooler operating points superimposed on the performance¹¹ of a typical BAe 50-80K cryocooler plotted versus stroke, input power, coldtip load, and coldtip temperature.

To estimate the level of load increase that occurred, one can examine representative curves¹¹ for the performance of the BAe 50-80K cooler as shown in Fig. 7. By plotting the MOPITT operating points on these curves it is seen that a stroke increase from 6.4 mm to 6.9 mm at the observed coldtip temperatures corresponds to a load increase of about 130 mW (8%) for cooler #1 and 230 mW (15%) for cooler #2. This is not too different from the ISAMS experience, although ISAMS chose to conduct its decontamination cycles at more frequent intervals.

BAe 80 K Cooler Life Test Experience

As a third example, a BAe 80 K cooler was life-tested in a vacuum bell jar at TRW in 1992 for around 160 days.¹² During this lifestest the chamber was maintained with a vacuum around 10^{-5} torr, and the cryocooler coldfinger was wrapped with multilayer insulation (MLI). As shown in Fig. 8, the coldtip experienced a continuous temperature increase over the lifestest period at a near-constant rate of 5.48 K/year. Similar to the ISAMS and MOPITT performance, the

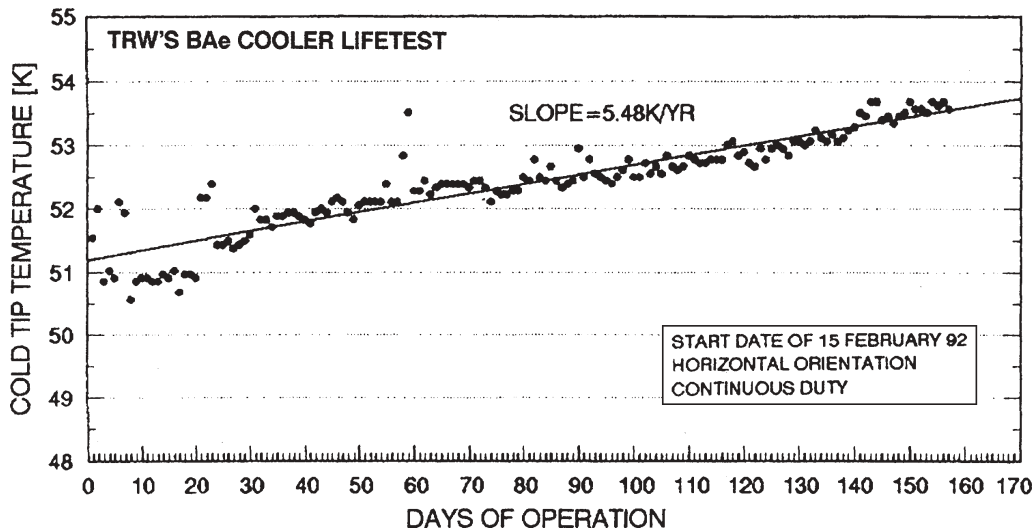


Figure 8. Performance degradation observed in lifetesting a BAe 80K cryocooler¹²; performance degradation was determined to be increased external radiation parasitics due to gettered contaminants; performance returned to normal after a room-temperature decontamination cycle.

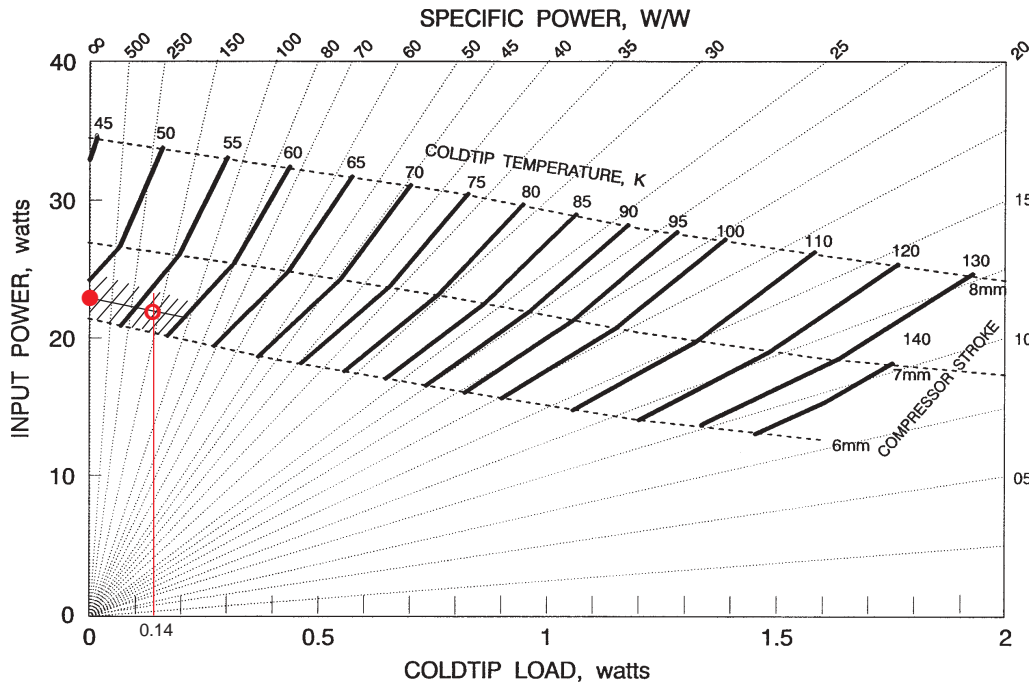


Figure 9. TRW lifestest data¹² superimposed on representative performance⁸ of a BAe 80K cryocooler plotted versus coldtip temperature, stroke, and input power for a 300K heatsink temperature.

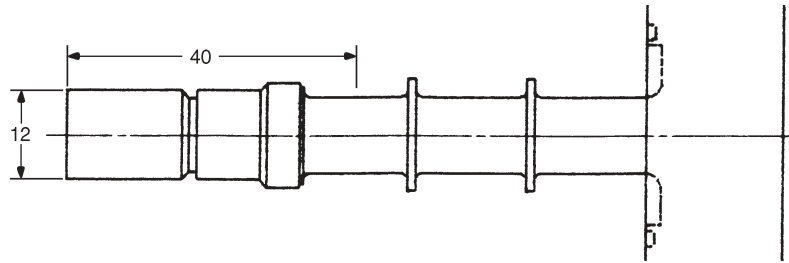


Figure 10. Scale drawing of the BAe 80K cryocooler coldfinger (dimensions are in mm); the estimated cryogenic surface area is approximately 25 cm².

performance degradation was traced to contamination of the external low-emittance thermal surfaces. From Fig. 9 it can be seen that 5.48 K/year at around 52 K equates to a radiation load increase of around 140 mW/year, again similar to the ISAMS and MOPITT experience.

To evaluate the load increase in terms of emittance increase requires the surface area of the cold surfaces and the temperature of the hot surrounds. Figure 10 is a scale drawing of the BAe 80K coldfinger from which the MLI area has been estimated to be around 25 cm². The bell jar was at room ambient (296 K). Solving for the increased emittance gives:

$$\begin{aligned}\Delta\epsilon &= \Delta Q / [5.67 \times \text{area} \times (T_H/1000)^4] \\ &= 0.14 \text{ W} / [5.67 \times 25 \text{ cm}^2 \times (296/1000)^4] \\ &= 0.13/\text{year}\end{aligned}$$

If, as opposed to MLI, this system had a single low emittance surface, Fig. 1 suggests that the emittance increase would amount to a single-surface ice film thickness growth of around 0.7 μm/year = 2.2×10⁻¹² cm/s. Similarly, for a single low-ε surface, Eq. 4 can be used to estimate what the background water vapor pressure would have had to be for this rate of film growth. Thus

$$P = 17.15 \dot{\delta} \rho \sqrt{T/M} = 17.15 (2.2 \times 10^{-12} \text{ cm/s})(0.9)(300/18)^{0.5} = 1.4 \times 10^{-10} \text{ torr} \quad (6)$$

Since this partial pressure of water is well below the expected vacuum chamber water vapor pressure, it suggests that using multilayer MLI is much better than a single low-emittance surface in controlling the effects of contamination. The data also suggest that to fully stabilize low

emissivity surfaces either requires very low partial pressures of water (say $< 10^{-12}$ torr), or more effective MLI involving many more layers that are kept contamination free. For ground life tests, one means of achieving a very low partial pressure of water is to shield the cryocooler coldend with a cryopumping shield with a temperature below around 120 K.

SUMMARY AND CONCLUSIONS

A brief review of the physics of cryocondensation has been presented to provide insight into the in-space cryocontamination issue and its effects on low-emittance surfaces. However, appropriate values for key parameters such as the effective partial pressure of water in a long-term space mission and the sensitivity of MLI to moisture film buildup are not readily available. As one means of estimating these unknown parameters, the in-space performance of some previous cryocooler-based space missions has been examined. Although the mission sample is small, the data indicate that around a 10-20% load increase may be expected on-orbit due to contamination of low- ϵ surfaces. This is for a typical cryogenic space instrument with a total cryogenic load on the order of one watt.

Historically, the established way to deal with this load increase has been to periodically boil off the contaminants by heating the cryogenic surfaces to near room temperature. This procedure has been found to work well, but the deep thermal cycling can also be very stressful to the systems involved. In addition, to provide sufficient cryocooler headroom to insure long uninterrupted operating periods between decontamination cycles, cryocoolers need to be appropriately oversized to accommodate this contamination-driven load increase.

In the future, it would be desirable to incorporate improved design features into cryogenic space applications that would greatly reduce or eliminate the degrading effects of on-orbit contamination. In the mean time, the issue of managing in-space contamination needs to be a focused part of the design and operation of any long-term cryogenic space application.

ACKNOWLEDGMENT

The work described in this paper was carried out at the Jet Propulsion Laboratory, California Institute of Technology, and was sponsored by the National Aeronautics and Space Administration.

REFERENCES

1. W. Viehmann and A.G. Eubanks, *Effects of Surface Contamination on the Infrared Emissivity and Visible-Light Scattering of Highly Reflective Surfaces at Cryogenic Temperatures*, NASA Technical Note TN D6585, NASA Goddard Space Flight Center, February 1972.
2. Barron, R.F., *Cryogenic Systems*, Oxford Univ. Press, New York, 1985, p. 225.
3. O'Hanlon, J.F., *A User's Guide to Vacuum Technology*, John Wiley & Sons, New York, 1989, p. 59.
4. Dushman, S. and Lafferty, J.M., *Scientific Foundations of Vacuum Technique*, John Wiley & Sons, New York, 1962, p. 14.
5. Barron, R.F., *Cryogenic Systems*, Oxford Univ. Press, New York, 1985, p. 455.
6. Boies, M. et al., "Measurement of long-term outgassing from materials used on the MSX spacecraft," *Proceedings of SPIE Vol. 4096 (2000)*, pp. 28-40.
7. ISAMS cooler data distributed by John Whitney, Oxford University Dept. of Physics, Oxford, UK, 1991-1993 (Private Communication).
8. Ross, R.G., Jr., Johnson, D.L., and Kotsubo, V.Y., *BAe 80K Stirling Cooler Performance Characterization*, JPL Internal Document D-9912, Jet Propulsion Laboratory, Pasadena, CA (1992).
9. Mand, G.S., Drummond, J.R., Henry, D., and Hackett, J., "MOPITT On-orbit Stirling Cycle Cooler Performance," *Cryocoolers II*, Kluwer Academic/Plenum Press, NY (2001), pp. 759-768.
10. MOPITT cryocooler year 2000 operations summary data distributed by G.S. Mand, Univ. of Toronto Dept. of Physics, Toronto, Canada, January 2001 (Private Communication).
11. Smedley, G.T., Mon, G.R., Johnson, D. L. and Ross, R.G., Jr., "Thermal Performance of Stirling-Cycle Cryocoolers: A Comparison of JPL-Tested Coolers," *Cryocoolers 8*, Plenum Publishing Corp., New York (1995), p. 187.
12. TRW's BAe Cooler Lifetest Data, distributed by Bill Burt, TRW, Redondo Beach, CA, 1992 (Private Communication).